

# Influence of Phenylethynylene of Push–Pull Zinc Porphyrins on the Photovoltaic Performance

Hsien-Hsin Chou,<sup>†</sup> Kamani Sudhir K. Reddy,<sup>†</sup> Hui-Ping Wu,<sup>‡</sup> Bo-Cheng Guo,<sup>†</sup> Hsuan-Wei Lee,<sup>†</sup> Eric Wei-Guang Diao,<sup>\*,‡</sup> Chao-Ping Hsu,<sup>\*,§</sup> and Chen-Yu Yeh<sup>\*,†</sup>

<sup>†</sup>Department of Chemistry and Research Center for Sustainable Energy and Nanotechnology, National Chung Hsing University, Taichung 402, Taiwan

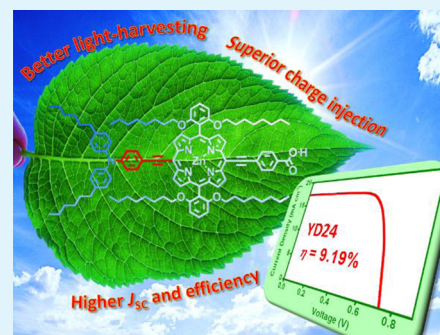
<sup>‡</sup>Department of Applied Chemistry and Institute of Molecular Science, National Chiao-Tung University, Hsinchu 300, Taiwan

<sup>§</sup>Institute of Chemistry, Academia Sinica, Taipei 115, Taiwan

## S Supporting Information

**ABSTRACT:** A series of zinc porphyrin dyes YD22–YD28 were synthesized and used for dye-sensitized solar cells. Dyes YD26–YD28 consist of zinc porphyrin (ZnP) as core unit, arylamine (Am) as electron-donating group, and *p*-ethynylbenzoic acid (EBA) as an electron-withdrawing/-anchoring group. The dyes YD22–YD25 contain additional phenylethynylene group (PE) bridged between Am and ZnP units. The influence of the PE unit on molecular properties as well as photovoltaic performances were investigated via photophysical and electrochemical studies and density functional calculations. With the insertion of PE unit, the dyes YD22–YD25 possess better light-harvesting properties in terms of significantly red-shifted Q-band absorption. The conversion efficiencies for dyes YD22–YD25 are better than those of dyes YD26–YD28 owing to larger  $J_{SC}$  output. Natural transition orbitals and Mulliken charge analysis were used to analyze the electron injection efficiency for porphyrin dyes upon time-dependent DFT calculations. The results indicated that insertion of additional PE unit is beneficial to higher  $J_{SC}$  by means of improved light-harvesting property due to broadened and red-shifted absorption.

**KEYWORDS:** charge transfer, density-functional, dye-sensitized solar cells, electron-donating, Mulliken charge, porphyrin sensitizers



## 1. INTRODUCTION

Solar energy is one of the most viable options for the increasing global energy demand. Among the many solar-to-electricity conversion techniques, dye-sensitized solar cells (DSCs) have attracted considerable attention because of their high absorption abilities to convert light-to-electricity, ease of fabrication, and low production cost.<sup>1,2</sup> The high-efficiency ruthenium polypyridyl dyes show power conversion efficiency of ca. 11% under standard global AM 1.5 (1 Sun) solar conditions with good stability.<sup>3–5</sup> However, the low absorption coefficient ( $\epsilon_{\max}$   $1\text{--}2 \times 10^4 \text{ M}^{-1}\text{cm}^{-1}$ ) and rareness of ruthenium-based dyes limit their wide application.<sup>6</sup> Organic dyes have also attracted great attention because of their modest cost, ease of synthesis, and modification with high absorption coefficients and promising stabilities.<sup>7–9</sup> However, DSCs based on organic dyes exhibited varied cell performances ranging from extremely poor to high as a result of slight modifications on molecular structures. Consequently, a great deal of effort has been made to search for new organic components for dye architecture to achieve high cell performance. Zinc porphyrin dyes, in contrast, play somewhat a compromising role in lieu of ruthenium-based and organic dyes. The syntheses and purifications for zinc porphyrin dyes can be as easy and competitive as those for organic dyes, and the device

performance and durability for porphyrin dyes can also rival both organic and ruthenium-based dyes.

Porphyrin dyes have the advantages of a highly absorptive Q-band and an intense Soret band. As inspired from natural antenna systems,<sup>10</sup> the advantage of the light-harvesting property of zinc porphyrin dyes in general is reflected in the high IPCE.<sup>11–13</sup> Like both ruthenium-based and organic dyes, upon rational molecular design, porphyrin-sensitized solar cells are capable of high cell performances.<sup>14–16</sup> In 2011, porphyrin YD2-o-C8<sup>17</sup> was reported to have a record-high conversion efficiency of 11.9%, which is superior to that of ruthenium dyes and organic dyes. In 2014, the structurally modified zinc porphyrin dyes GY50 and SM315 again recorded the highest conversion efficiencies of 12.5 and 13.0%, respectively.<sup>18,19</sup> It is thus desirable to understand the structure–property relationships of zinc porphyrin dyes.

Porphyrin sensitizers with 4 meso and 8 beta positions can be easily modified to fine-tune the photophysical and electrochemical properties and to achieve high performance of the photovoltaic devices. It is well-known that the planar

Received: November 27, 2015

Accepted: January 11, 2016

Published: January 11, 2016

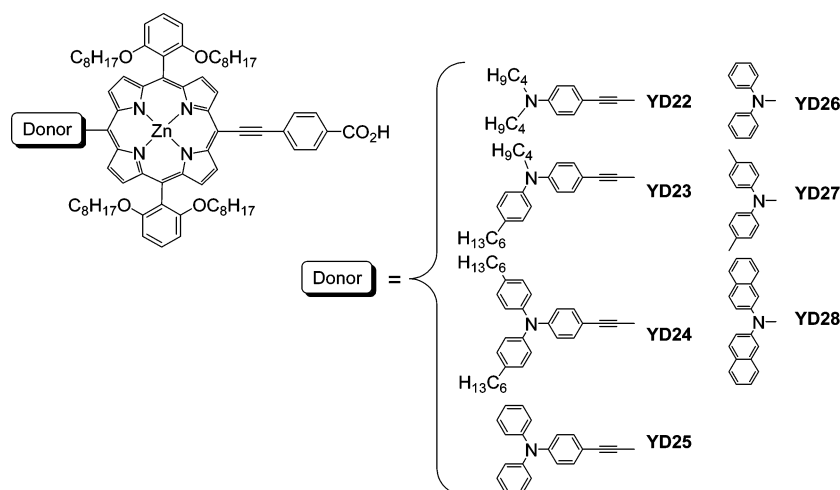


Figure 1. Design of porphyrin sensitizers.

feature of porphyrins tend to form  $\pi$ -stacked aggregates, which significantly deteriorates electron injection to  $\text{TiO}_2$  surface. Introduction of aryl moieties with ortho-substituted alkoxy chains on meso positions of porphyrin moiety can reduce dye aggregation and suppress the electron transfer from  $\text{TiO}_2$  conduction band to electrolyte.<sup>20,21</sup> It is also found that the performance of porphyrin-based sensitizers can be dramatically improved by utilizing appropriate donor and acceptor groups. Our previous studies indicate that donor moieties are one of the key factors influencing the light-harvesting ability and charge separation between the porphyrin dye and  $\text{TiO}_2$  conduction band.<sup>22–25</sup> Utilizing *N,N*-diaryl-substituted amines as the donor is beneficial to facilitate charge separation and give high device performance.<sup>22,23,25–29</sup> In addition, the ethynylene group of ethynyl benzoic acid (EBA) entity bridges between the anchor and porphyrin is able to mediate the electronic communication efficiently. This efficient conjugation system is expected to improve the cell performance by means of enhanced light-harvesting property and electron transfer from the excited state of the dyes to the  $\text{TiO}_2$  surface. Examples such as YD-series dyes with zinc porphyrin core simultaneously containing *meso*-10,20-bis(alkoxyaryl), *meso*-5-(diaryl)amino, and *meso*-15-ethynyl benzoic acid moieties have impressively high device performances.<sup>22,30,31</sup> In an attempt to improve the efficiencies further, some studies reported by us<sup>23,31</sup> and other groups<sup>28,32–38</sup> also involve an additional phenylethynylene (PE) group in the conjugation backbone. Promising device performances were found because of elongation of  $\pi$  conjugation and released steric hindrance. Herein we reported two series of zinc porphyrin sensitizers, e.g., the dyes YD22–YD28, with and without additional PE group, respectively (Figure 1). The synthesis, optical behavior, and photovoltaic properties of dyes were elaborated, and the role of PE group was investigated by means of photophysical, electrochemical, and time-dependent DFT approaches.

## 2. EXPERIMENTAL SECTION

**2.1. General Information.** All reagents and solvents were obtained from commercial sources and used without further purification unless otherwise noted.  $\text{CH}_2\text{Cl}_2$  was dried over  $\text{CaH}_2$  and freshly distilled before use. THF was dried over sodium/benzophenone ketyl and freshly distilled prior to use. Tetra-*n*-butylammonium hexafluorophosphate ( $[(n\text{-Bu})_4\text{N}]\text{PF}_6$ ) was recrystallized twice from absolute ethanol and further dried for 2 days under

vacuum. Column chromatography was carried out on silica gel (Merck, 70–230 Mesh ASTM).  $^1\text{H}$  and  $^{13}\text{C}$  NMR spectra were acquired on a Varian spectrometer operating at 400 and 100 MHz, respectively. The UV–visible absorption and emission spectra were measured using a Varian Cary 50 spectrophotometer and JASCO FP-6000 spectrofluorometer, respectively. FAB-MS mass spectra were recorded on Bruker APEX II spectrometer operating in the positive ion detection mode. Electrochemical tests were carried out on CH Instruments 750A potentiostat using deoxygenated THF as solvent. A standard cyclic voltammetric (CV) experiment based on a three-electrode system is conducted. The working electrode uses a BAS glassy carbon ( $0.07\text{ cm}^2$ ) disk, whereas the reference and auxiliary electrodes used Ag/AgCl (saturated) and platinum wire, respectively. Potentials are reported with reference to ferrocene/ferrocenium ( $\text{Fc}/\text{Fc}^+$ ) couple at  $E_{1/2} = +0.63\text{ V}$  vs NHE at  $23\text{ }^\circ\text{C}$  in THF. The working electrode was polished with  $0.03\text{ }\mu\text{m}$  aluminum on felt pads (Buehler) and treated ultrasonically for 1 min before each experiment. The reproducibility of individual potential values was within  $\pm 5\text{ mV}$ .

**2.2. Synthesis.** The synthesis procedures and characterizations of compounds zinc(II) 5,15-bis(2,6-dioctyloxyphenyl)-10-bromoporphyrin (A), zinc(II) 5,15-bis(2,6-dioctyloxyphenyl)-10,20-dibromoporphyrin (A'), zinc(II) 5,15-bis(2,6-dioctyloxyphenyl)-10,20-(bis-(triisopropylsilyl)ethynyl)porphyrin (B),<sup>39</sup> zinc(II) 5,15-bis(2,6-dioctyloxyphenyl)-10-((triisopropylsilyl)ethynyl)porphyrin (C), zinc(II) 5,15-bis(2,6-dioctyloxyphenyl)-10-((triisopropylsilyl)ethynyl)-20-(bis-(aryl)amino)porphyrin (D<sub>26</sub>–D<sub>29</sub>) and dyes YD22–YD28 are described in the Supporting Information or literature as noted.

**2.3. Assembly and Characterization of DSCs.** The photoanode used was the  $\text{TiO}_2$  thin film ( $3\text{ }\mu\text{m}$  of 25 nm particles and  $9\text{ }\mu\text{m}$  of 100 nm nanorods as the dye adsorption layers and  $6\text{ }\mu\text{m}$  of 400 nm particles as the light-scattering layer) coated on an FTO glass substrate with a dimension of  $0.4 \times 0.4\text{ cm}^2$ , and the film thickness was measured by a profilometer (Dektak3, Veeco/Sloan Instruments Inc., USA). A platinized FTO produced by thermopyrolysis of  $\text{H}_2\text{PtCl}_6$  was used as a counter electrode. The  $\text{TiO}_2$  thin film was dipped into the ethanol solution containing  $2 \times 10^{-4}\text{ M}$  dye sensitizers and  $1 \times 10^{-3}\text{ M}$  chenodeoxycholic acid (CDCA) for at least 12 h. After rinsing with ethanol, the photoanode and the counter electrode were sealed at  $90\text{ }^\circ\text{C}$  with a  $0.25\text{ cm}^2$  hollowed melting film (Surllyn 1706/thickness  $60\text{ }\mu\text{m}$ , DuPont, USA) The electrolyte was then injected into the space between the two electrodes through the filling hole on FTO and sealed with Surllyn film and coverglass. The electrolyte was composed of 0.1 M lithium iodide (LiI), 0.05 M iodine ( $\text{I}_2$ ), 1 M 1-propyl-3-methylimidazolium iodide (PMII), and 0.5 M 4-*tert*-butylpyridine that was dissolved in a mixture of acetonitrile and valeronitrile (in 85:15 volume ratio).

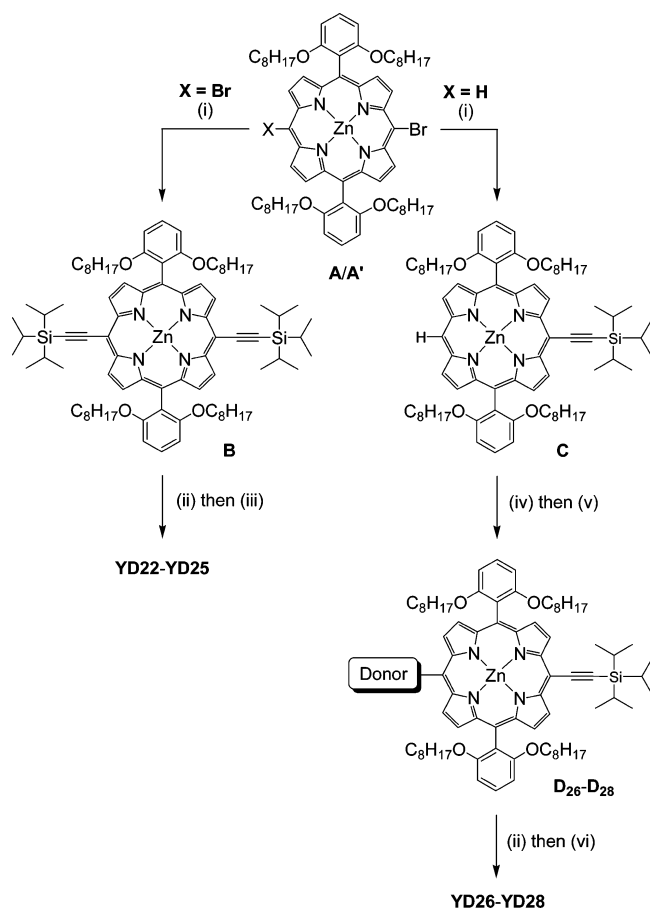
**2.4. Quantum Chemistry Computation.** The computations were carried out with developed version of Q-Chem 4.0 software.<sup>40</sup>

The long-range corrected (LRC) functional  $\omega$ PBE<sup>41,42</sup> was employed for all the calculations in the present study. The range-separation parameter  $\omega$  was set to 0.12 au following the scheme described in the literature.<sup>43</sup> The 6-31G(d) basis set was used for all atoms excepted for Zn, where CRENBL basis set with core electrons described via pseudopotential was employed. All the aliphatic chains were replaced with  $-\text{CH}_3$  group in order to save computational effort. Geometry optimization of the molecules was carried out prior to further calculations. Mulliken charge analysis on the basis of time-dependent density functional (TDDFT) calculations were carried out according to established protocols.<sup>44–46</sup>

### 3. RESULTS AND DISCUSSION

**3.1. Synthesis of Materials.** The synthesis of YD-series dyes including asymmetric functionalization of porphyrin followed the established routes as reported earlier.<sup>24,31,47</sup> The synthesis routes for these porphyrin dyes are summarized in Scheme 1 and detailed in the Experimental Section and

Scheme 1. Synthesis Routes for Porphyrin Dyes<sup>a</sup>



iodophenyl)diarylamine and *p*-iodobenzoic acid via Sonogashira coupling to give product YD22–YD25 in 32–45% yields. Similarly, bromination of C at *meso*-5-position was conducted to obtain the asymmetric intermediate, which further underwent palladium-catalyzed Buchwald–Hartwig coupling<sup>49,50</sup> with an appropriate diarylamine to afford D<sub>26</sub>–D<sub>29</sub>. Deprotection at the ethynyl group and further Sonogashira coupling with *p*-iodobenzoic acid gave the product YD26–YD28 in 81–84% yields. All YD-series dyes are air-stable and readily soluble in common organic solvent such as CH<sub>2</sub>Cl<sub>2</sub>, THF, acetone, and acetonitrile.

**3.2. Photophysical Properties.** Figure 2 displays the UV–vis absorption spectra for YD-series dyes, and the correspond-

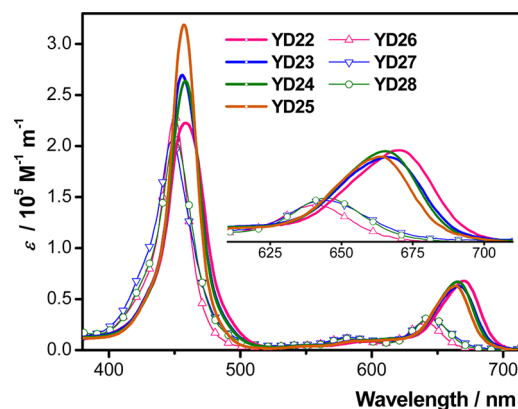


Figure 2. Absorption spectra of YD-series dyes in THF. Inset shows magnification of the Q-band signals.

ing parameters are summarized in Table 1. These dyes have intensive Soret band at 400–500 nm ( $\epsilon = 205\,000\text{--}315\,000\text{ M}^{-1}\text{ cm}^{-1}$ ) due to characteristic  $\pi\text{--}\pi^*$  transition predominantly localized at porphyrin ring. Moderate Q-band with strong charge-transfer character is also observed (ca. 550–700 nm;  $\epsilon = 26\,000\text{--}68\,000\text{ M}^{-1}\text{ cm}^{-1}$ ) for these push–pull-type dyes. The peak maxima of Soret bands for porphyrin dyes are centered at 444–459 nm. Apparently, variation of the diarylamino group does not significantly affect the high-energy transitions. In contrast, the Q-bands ( $\lambda_{\text{max}}$ ) are reasonably correlated with the donating ability of the amine donor featuring stronger electron-donating alkyl than that of aryl substituents. This result is of the trend YD25 (diphenyl; 663 nm) < YD24 (dihexylphenyl; 665 nm) < YD23 (*p*-hexylphenyl and *n*-butyl; 666 nm) < YD22 (bis(*n*-butyl); 671 nm) for *N,N*-disubstituted-4-(*p*-ethynylphenyl)aniline donor and YD26 (diphenyl; 641 nm) < YD27 (bis(*p*-tolyl); 644 nm) < YD28 (bis(2-naphthyl); 646 nm) for diarylamine donor. Note a second phenylethynylene unit (PE) bridged between ZnP and donor moieties is found to shift the Q-band absorption both bathochromically and hyperchromically. This is seen in the comparison of YD25 to YD26 ( $\lambda_{\text{max}}$ : 663 vs 641 nm;  $\epsilon$ :  $6.3 \times 10^4$  vs  $2.7 \times 10^4\text{ M}^{-1}\text{ cm}^{-1}$ ) and of YD24 to YD27 ( $\lambda_{\text{max}}$ : 665 vs 644 nm;  $\epsilon$ :  $6.8 \times 10^4$  vs  $3.1 \times 10^4\text{ M}^{-1}\text{ cm}^{-1}$ ). This behavior is not considered a consequences of stronger charge-transfer (CT) character in YD22–YD25. However, it is suggested that the PE-containing dyes have more pronounced transition moment and smaller transition energy due to extended  $\pi$  conjugation. The same phenomenon was also observed in the case of YD7 versus YD3.<sup>22</sup> It is also noted that the position of the inserted PE unit is also important to relative intensity and absorption maxima of

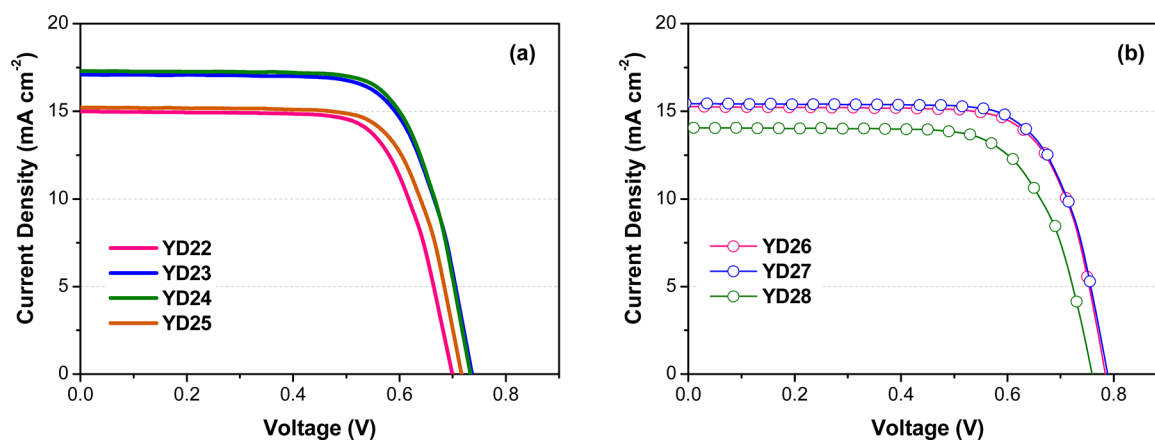
**Supporting Information.** The mono- (A) and bis-brominated porphyrin (A') first underwent palladium-catalyzed Sonogashira coupling<sup>48</sup> with triisopropylsilyl acetylene (TIPSA) to give B and C, respectively, in moderate yields. Deprotection of B in the presence of fluoride gave bis(ethynyl)-substituted zinc porphyrin intermediate, which was reacted with (*p*-



Table 1. Photophysical and Electrochemical Data for YD-Series Dyes

dye	$\lambda_{\max}$ ( $\epsilon$ ) (nm and $10^3 \text{ M}^{-1} \text{ cm}^{-1}$ ) <sup>a</sup>	$\lambda_{\text{em}}$ (nm) <sup>b</sup>	$E_{0-0}$ (eV) <sup>c</sup>	$\nu_{\text{st}}$ ( $\text{cm}^{-1}$ ) <sup>d</sup>	$E_{1/2}^{\text{ox}}/E_{1/2}^{\text{red}}$ (V/V) <sup>e</sup>	$E_{0-0}^*$ (V) <sup>f</sup>
YD22	459 (223), 671 (68)	676	1.84	110	+0.78, +1.02/−1.21	−1.06
YD23	456 (268), 666 (63)	686	1.83	438	+0.81, +1.09/−1.23	−1.02
YD24	459 (269), 665 (68)	673	1.85	179	+0.87, +1.16/−1.16	−0.98
YD25	456 (315), 663 (63)	703	1.83	858	+0.88, +1.19/−1.18	−0.95
YD26	449 (229), 579 (11), 641 (27)	657	1.91	380	+0.86, +1.37/−1.29	−1.05
YD27	448 (205), 582 (13), 644 (31)	666	1.90	513	+0.82, +1.34/−1.29	−1.08
YD28	450 (208), 582 (11), 646 (32)	659	1.91	305	+0.85, +1.37/−1.27	−1.06

<sup>a</sup>Absorption is measured in THF at 25 °C. <sup>b</sup>Emission is measured in THF at 25 °C using the longest wavelength absorption maximum as excitation wavelength. <sup>c</sup>Optical bandgap ( $E_{0-0}$ ) is obtained from cross point of normalized  $\lambda_{\max}$  and  $\lambda_{\text{em}}$ . <sup>d</sup>Stokes shift. <sup>e</sup>Redox potentials are measured in THF containing 0.1 M [(*n*-Bu)<sub>4</sub>N]<sup>+</sup>PF<sub>6</sub><sup>−</sup> as supporting electrolyte. Potentials are quoted with Ag/AgCl reference electrode using ferrocene/ferrocenium (Fc/Fc<sup>+</sup>) couple as internal standard and are converted to that vs normal hydrogen electrode (NHE) by addition of +0.63 V. <sup>f</sup>Zero-zero excitation energy ( $E_{0-0}^*$ ) is obtained from redox potential and optical bandgap ( $E_{0-0}$ ).

Figure 3. *J*–*V* plots of (a) PE-containing and (b) PE-free dyes.

Q-band of zinc porphyrin dyes. The reported dye LAC-1<sup>34</sup> (629 nm;  $4.72 \times 10^4 \text{ M}^{-1} \text{ cm}^{-1}$ ) with PE implanted between zinc porphyrin and *p*-ethynylbenzoic acid (EBA) has a more blue-shifted Q-band absorption than that of similar derivative compound 4 (668 nm;  $5.10 \times 10^4 \text{ M}^{-1} \text{ cm}^{-1}$ )<sup>23</sup> and YD25 in this study. Extended  $\pi$  conjugation on diarylamine also increases the donor ability of the diarylamine and pushes the Q-band bathochromically, e.g., YD28 (646 nm,  $3.2 \times 10^4 \text{ M}^{-1} \text{ cm}^{-1}$ ) versus YD26. Obviously, both  $\pi$  extension and alkyl introduction onto the donor group perturbs the HOMO level toward higher energy because of the reason that on the basis of four-orbital theory<sup>31</sup> the  $a_{2u}$  orbital involved in the Q-band of porphyrin is largely affected by meso substituents.

All the YD-series dyes show emission ranging from 639 to 686 nm. The Stokes shifts (110–858  $\text{cm}^{-1}$  for YD22–YD25; 305–513  $\text{cm}^{-1}$  for YD26–YD28) of these dyes were found to be relatively small compared to those of some metal-free dipolar organic dyes,<sup>45,52–54</sup> indicating a smaller energy required for geometrical reorganization of push–pull porphyrin dyes at photoexcited state.

**3.3. Electrochemical Properties.** Cyclic voltammetry was carried out to determine the redox potentials of the dyes in THF, and the results are depicted in Figure S1 and Table 1. The YD-series dyes exhibit reversible oxidation and reduction potentials. These dyes have two oxidation potentials located at ca. +0.8 V and ca. +1.2 to +1.3 V, which indicates that oxidation happens at arylamino donor and at the zinc porphyrin unit, respectively.<sup>22,23</sup> The first oxidation potentials for YD-series dyes is strongly correlated with the substituents on arylamino donor: YD22 (bis(*n*-butyl), +0.78 V) < YD23 (*p*-hexylphenyl

and *n*-butyl, +0.81 V) < YD24 (bis(*p*-hexylphenyl), +0.87 V)  $\approx$  YD25 (biphenyl, +0.88 V); YD27 (bis(*p*-tolyl), +0.82 V) < YD28 (bis(2-naphthyl), +0.85 V) < YD26 (biphenyl, +0.86 V). With the same bis(*p*-tolyl)amino donor, YD24 (0.87 V) has larger oxidation potential and thus lower HOMO level than that of YD27 (0.82 V). The same observation was found in the case of diphenyl amino derivatives, e.g., YD25 (0.88 V) versus YD26 (0.86 V). Consequently, the HOMO energy level, which is primarily originated from electron-donating ability of amine, is much stabilized by the PE-bridged porphyrin in the case of YD22–YD25. In other words, the additional phenylethynylene unit (PE) facilitates the electronic communication between amino donor and zinc porphyrin. This phenomenon is also evident in the LUMO level of the dyes. As listed in Table 1, only one reduction potential (ca. −1.2 V) is observed in the electrochemical window of THF, representing the electron-accepting ability of EBA unit. The excited-state potentials ( $E_{0-0}^*$ ) are relatively lower for dyes YD22–YD25 (−1.16 to −1.23 V) than those for YD26–YD28 (−1.27 to −1.29 V), showing the influence of additional phenylethynylene group. According to the results, all YD-series dyes have sufficiently high LUMO level as opposed to TiO<sub>2</sub> conduction band Fermi level (−0.5 V vs NHE),<sup>4,5</sup> which allows effective charge injection. In contrast, the large difference between redox potentials of YD-series dyes and I<sup>−</sup>/I<sub>3</sub><sup>−</sup> (ca. 0.4 V vs NHE)<sup>55–57</sup> also indicates favored driving force for dye regeneration of the former after electron injection.

**3.4. Device Performances.** The porphyrin dyes synthesized in this work were fabricated as dye-sensitized solar cells. Iodine/triiodide in a mixed solvent of ionic liquid (1-methyl-3-

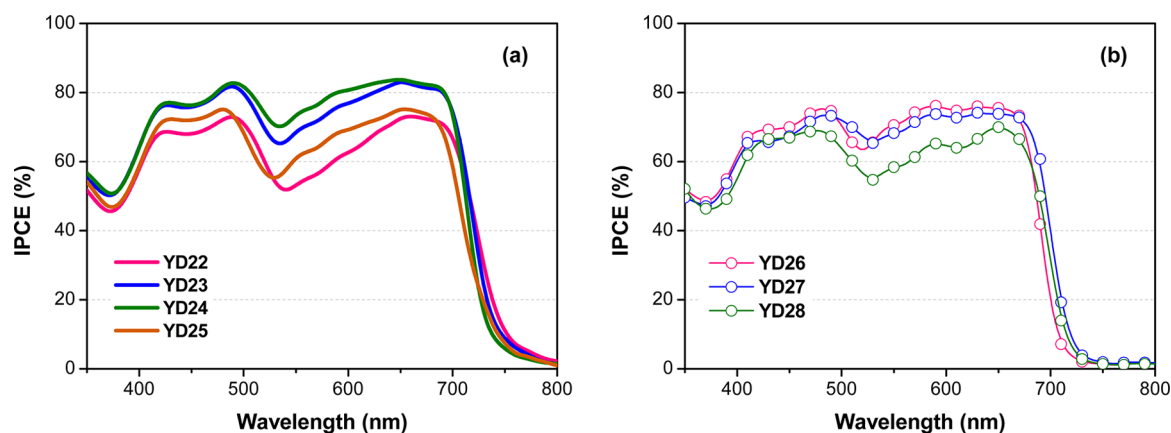


Figure 4. IPCE plots of (a) PE-containing and (b) PE-free dyes.

propylimidazolium iodide, PMII), acetonitrile, and valeronitrile are used as redox electrolyte throughout the study. The results are displayed in Figures 3 and 4, and the parameters are summarized in Table 2. Devices fabricated with the porphyrin

Table 2. Device Performance of YD-Series Dyes

dye	$V_{OC}$ (V)	$J_{SC}$ ( $\text{mA cm}^{-2}$ ) <sup>a</sup>	FF	$\eta$ (%)	dye loading $\times 10^{-9}$ ( $\text{mol cm}^{-2}$ )
YD22	0.70	14.92 (14.37)	72.43	7.56	126.7
YD23	0.74	17.10 (16.40)	71.41	9.00	160.5
YD24	0.73	17.29 (16.61)	72.46	9.19	130.4
YD25	0.72	15.22 (14.76)	72.66	7.93	148.1
YD26	0.79	15.26 (13.97)	73.24	8.79	125.7
YD27	0.79	15.45 (14.19)	73.07	8.92	99.7
YD28	0.76	14.07 (12.74)	70.60	7.58	105.1

<sup>a</sup>The values shown in parentheses were obtained from integration of IPCE with standard solar photon flux spectra.

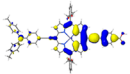
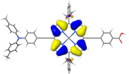
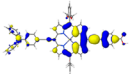
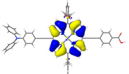
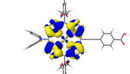
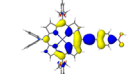
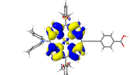
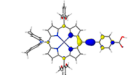
dyes have comparable open-circuit voltage ( $V_{OC}$ : 0.70–0.79 V) and short-circuit current ( $J_{SC}$ : 14.07–17.29  $\text{mA cm}^{-2}$ ). As shown in Figure 3, derivatives YD22–YD25 have slightly lower  $V_{OC}$  (0.70–0.74 V) but are of roughly higher current output (14.92–17.29  $\text{mA cm}^{-2}$ ) than are YD26–YD28 (0.76–0.79 V; 14.07–15.45  $\text{mA cm}^{-2}$ ) (Figures 3 and 4). This phenomenon is

believed to stem from better charge injection ability of PE-containing dye YD22–YD25. It is suggested that the  $\text{TiO}_2$  electron quasi-Fermi-level is changed because of changing of interfacial recombination rate of  $\text{TiO}_2$  electrons with electrolytes/dye cation.<sup>58–61</sup> This phenomenon is believed to arise from structural modulation. We tentatively assumed that for YD22–YD25 the lower dye LUMO levels stemmed from additional PE group leads to downward shift of  $\text{TiO}_2$  conduction band edge which results in the decrease in  $V_{OC}$  increase in charge density.<sup>62,63</sup> Therefore, involvement of the PE group leads to the downward shift of the  $\text{TiO}_2$  conduction band edge, resulting in the lowering down of the Fermi level of  $\text{TiO}_2$  and thus decreasing the  $V_{OC}$  as we observed for devices made of YD22–YD25. With the presence of 5 equiv of CDCA coadsorbent, the observed  $J_{SC}$  for each dyes slightly decreased for 3–9% probably because of decreased occupation sites for porphyrin dyes. Like that in the CDCA-free case, the  $J_{SC}$  values are larger for dyes YD22–YD25 (14.37–16.61  $\text{mA cm}^{-2}$ ) than those for YD26–YD28 (12.74–14.19  $\text{mA cm}^{-2}$ ). The generally higher photocurrent output for dyes having additional PE unit is ascribed to better light-harvesting property and enhanced injection ability due to the downward shift of the conduction band edge of  $\text{TiO}_2$ , giving more driving force for electron injection. It is also noted that the reported dye YD7 ( $V_{OC}$  = 0.65 V;  $J_{SC}$  = 10.05  $\text{mA cm}^{-2}$ ;  $\eta$  = 4.38%) with an additional PE

Table 3. Calculated Results for Q-Band ( $S_0 \rightarrow S_1$ ) Transitions and NTOs of Select Dyes

Dye	$E_{cal}$ (eV)	$f$	$ f^2 \Delta q_{Ac} $	NTO (Particle $\rightarrow$ Hole)			
				Major contribution		Minor contribution	
YD24	1.90	0.95	0.007		78%		18%
YD25	1.91	0.91	0.006		78%		19%
YD26	1.95	0.37	0.002		79%		19%
YD27	1.91	0.38	0.003		81%		16%

Table 4. Calculated Results for Major Soret Band Transitions and NTOs of Selected Dyes

Dye	$E_{\text{cal}}$ (eV)	$f$	$ f \times \Delta q_{\text{Ac}} $	NTO (Particle $\rightarrow$ Hole)			
				Major contribution		Minor contribution	
<b>YD24</b> ( $S_0 \rightarrow S_7$ )	2.96	1.08	0.044		48%		36%
<b>YD25</b> ( $S_0 \rightarrow S_7$ )	2.97	0.96	0.036		52%		33%
<b>YD26</b> ( $S_0 \rightarrow S_7$ )	2.92	1.24	0.036		56%		26%
<b>YD27</b> ( $S_0 \rightarrow S_7$ )	2.91	1.30	0.042		55%		27%

unit has device performance slightly poorer than that of PE-free dye YD3 ( $V_{\text{OC}} = 0.71$  V;  $J_{\text{SC}} = 10.85$  mA cm $^{-2}$ ;  $\eta = 5.34\%$ ).<sup>22</sup> The discrepancy between systems in this study and the earlier report probably comes from different peripheral substituents on zinc porphyrin group. Unlike the 2,6-bis(octyl)phenyl group, the 3,5-bis(*tert*-butyl)phenyl group is unable to effectively block the electrolyte from approaching the TiO $_2$  surface in the case of YD7. In contrast, the sterically demanding diphenylamino group directly attached to zinc porphyrin in YD3 is beneficial to suppression of dye aggregation, leading to higher performance.<sup>17</sup>

**3.5. Theoretical Investigations.** To evaluate the role of the phenylethynylene group in high-performance pull-pull-type zinc porphyrin dyes, theoretical studies were conducted. The gas-phase density functional (DFT) calculations were carried out with long-range-corrected  $\omega$ PBE functional. To save computational costs, all the alkoxy and alkyl chains were replaced by methoxy and methyl groups, respectively. The discussions of frontier orbitals from ground-state DFT results were elucidated in the [Supporting Information](#).

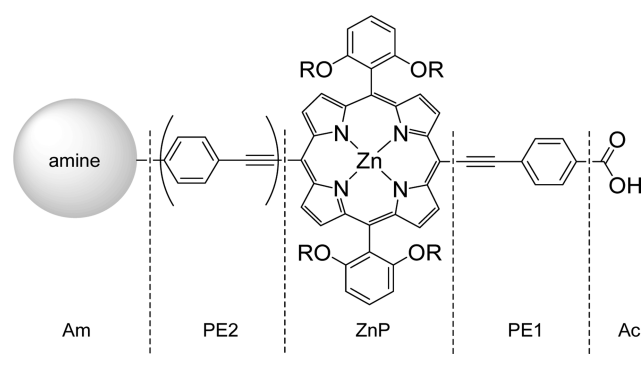
With TDDFT calculations, we have studied the excitation of YD-series dyes. The corresponding natural transition orbitals (NTOs) and Mulliken charge analyses were carried out. NTO is a compact representation of pairs of particle and hole orbitals for a given electronic transition. This simplifies the qualitative analysis of vertical excitation behavior, where multiple HOMO–LUMO components are often observed in most transitions. In [Tables 3](#) and [4](#) as well as [Tables S1](#) and [S2](#), we summarized the parameters of excitation, including calculated transition energy ( $E_{\text{cal}}$ ), oscillator strength ( $f$ ), and NTOs specifically corresponding to the Q-band ( $S_0 \rightarrow S_1$ ) and major Soret band (usually  $S_0 \rightarrow S_7$ ) transitions of YD-series dyes. For the Q-band transitions, the major components of particle-to-hole NTOs (77–81%) for all dyes generally represent a localized excitation (LE) property with a strong CT character. However, the minor components in NTOs (16–19%) are localized  $\pi$ – $\pi^*$  transitions at ZnP moiety. Consequently, in the YD-series dyes, the efficient injection of electrons is mainly due to large component of CT character in the Q-band transitions. It is noted that the PE-containing dyes YD22–YD25 exhibit larger oscillator strength ( $f = 0.80$ – $0.95$ ) from ground to first

excited states ( $S_0 \rightarrow S_1$ ) than those of PE-free dyes YD26–YD28 ( $f = 0.37$ – $0.38$ ), due to elongated  $\pi$  conjugation with the PE and better particle–hole orbital overlap in the transition in the former. This result is also in good agreement with more intensive Q-band absorptions in UV–vis spectra observed for dyes YD22–YD25.

Transitions with the largest oscillator strength ( $S_0 \rightarrow S_6$  for YD28 and  $S_0 \rightarrow S_7$  for all the rest) are calculated to be ca. 1 eV higher in energy than Q-band transitions. (Detailed results are listed in [Table S2](#).) These states are of large oscillator strengths ( $f = 0.83$ – $1.69$ ) and are assigned as the predominant Soret band. Together with other considerably strong transitions at similar energies ( $S_0 \rightarrow S_n$ , where  $n = 3$ – $10$ ), the convoluted Soret bands for these dyes are expected to be of extremely high intensity, contributing to the large extinction coefficients of the band. We note that for PE-containing dyes YD22–YD25 the major NTO component (48–57%) is mainly a local excitation in ZnP and PE with CT character toward the acceptor. This CT character is relatively small in numerical analysis and it is not clearly visible in the NTOs ([Table S2](#) and [S3](#)). The minor component is localized  $\pi$ – $\pi^*$  transitions at ZnP. For the PE-free dyes YD26–YD28, on the contrary, only the minor NTO pairs are the ZnP–PE excitation with a small CT character, with their population ranging from 26 to 33%, and the major component is the localized  $\pi$ – $\pi^*$  transitions at ZnP. It is thus reasonable to conclude that PE-containing dyes are slightly more able to inject an electron into TiO $_2$ , with the small CT character in Soret band. It is noted that there exists internal conversion for zinc porphyrin from  $S_2$  (Soret band) to  $S_1$  (Q-band) state;<sup>65–67</sup> therefore, we cannot rule out the possibility of charge injection by this pathway. Introduction of an additional PE between arylamine donor and ZnP not only narrows the absorption bandgap (via elongation of  $\pi$  conjugation) but also modulates the CT characteristics of charge excitation.

To see better the extent of CT in the excitations, we have calculated the Mulliken charges for each atom, in both ground and excited states. The charge differences ( $\Delta q$ ) are grouped into five fragments including arylamine (Am), the attached phenylethynylene linker (PE2), zinc porphyrin (ZnP), the phenylethynylene linker to the acceptor (PE1), and carboxylic acid (Ac; [Scheme 2](#)). With similar analyses, it has been found

Scheme 2. Segmentation of Molecular Structure for YD-Series Dyes



that dipolar organic dyes with D- $\pi$ -A- $\pi$ -A' framework are likely to have strong CT transition with significant accumulation of positive charge at arylamine donor (D) and negative charge at electron-acceptor (A/A').<sup>44,68</sup> In Figure 5 we show  $\Delta q$  for each partitioned group between ground and excited states of YD-series dyes. The results clearly differentiate the Q-band and the major Soret band transitions within dyes in this study. As shown in Figure 5a, upon Q-band transition the Am group ( $\Delta q_{Am} = 0.020$ – $0.034$  for YD22–YD25;  $0.241$ – $0.328$  for YD26–YD28) and PE2 group ( $\Delta q_{PE2} = 0.043$ – $0.069$  for YD22–YD25) collect mostly positive charge, whereas the ZnP group ( $\Delta q_{ZnP} = -0.057$  to  $-0.070$  for YD22–YD25;  $-0.216$  to  $-0.294$  for YD26–YD28) collects negative charge. This indicates the donor ability of Am group (and, to some extent, the PE2 group) as well as the acceptor ability of ZnP group. Accordingly, in the Q-band transitions, CT takes place between Am/PE2 and ZnP groups, and this CT is more prominent in PE2-free dyes. Meanwhile, there is only a minimum amount of charge accommodation at the Ac group ( $\Delta q_{Ac} = -0.007$  to  $-0.008$ ) compared to that in the ZnP group. Similar behavior is observed for major Soret band transitions (Figure 5b). However, in this case, the Ac group accommodates more negative charge ( $\Delta q_{Ac} = -0.038$  to  $-0.046$  for YD22–YD25;  $-0.029$  to  $-0.037$  for YD26–YD28) than does the ZnP group compared to that in Q-band transition.

It is known that the short-circuit current is proportional to a product of light-harvesting efficiency ( $\eta_{LH}$ ), charge injection efficiency ( $\eta_{inj}$ ), and charge collection efficiency ( $\eta_{col}$ ):<sup>69</sup>

$$J_{SC} = q \int \eta_{LH}(\lambda) \eta_{inj}(\lambda) \eta_{col}(\lambda) I(\lambda) d\lambda \quad (1)$$

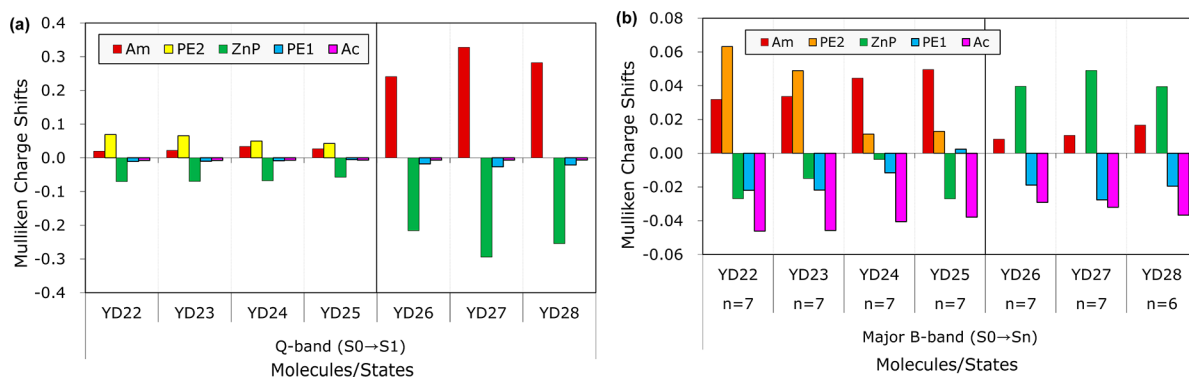


Figure 5. Differences in Mulliken charge population of (a) Q-band and (b) major Soret band transitions for YD-dyes.

It is thus reasonable to model  $\eta_{inj}$  by the amount of negative charge at the anchoring group in an excitation. With this in mind, the product of  $\eta_{LH}$  and  $\eta_{inj}$  can be ideally interpreted as the product of oscillator strength and Mulliken charge collected at Ac group, namely,  $f \times \Delta q_{Ac}$ . Previous study has shown a reasonable correlation between calculated  $|f \times \Delta q_{Ac}|$  value and short-circuit current ( $J_{SC}$ ) in dipolar organic dyes with D- $\pi$ -A- $\pi$ -A' framework, where D and A/A' represents donor and acceptors, respectively.<sup>46</sup> The calculated  $|f \times \Delta q_{Ac}|$  values for dyes in this study are included in Table 3 and 4. The PE2-containing dyes have larger oscillator strengths, as seen in the larger  $|f \times \Delta q_{Ac}|$  for Q-band transition (YD22–YD25: 0.006–0.007) compared to those in PE2-free cases (YD26–YD28: 0.002–0.003). Interestingly, with the same bis(*p*-tolyl)amino donor, the PE2-containing YD24 has a larger  $|f \times \Delta q_{Ac}|$  value than that of PE2-free YD27 for both Q-band transition (0.007 vs 0.003) and major Soret band transition (0.044 vs 0.042). The PE2-moiety increases charge injection by increasing the  $\pi$  conjugation; consequently, the oscillator strength is increased, leading to higher absorption that contributes to  $J_{SC}$ . A similar observation is also seen in dyes bearing diphenylamino donor. The PE2-containing dye YD25 has larger  $|f \times \Delta q_{Ac}|$  value and higher  $J_{SC}$  compared to those of PE2-free dye YD26.

To probe better the information concerning dyes after charge injection, the ground-state optimization of cationic dyes was carried out at same theoretical level and the charge distributions in which the cationic dyes were analyzed. In Figure 6, the

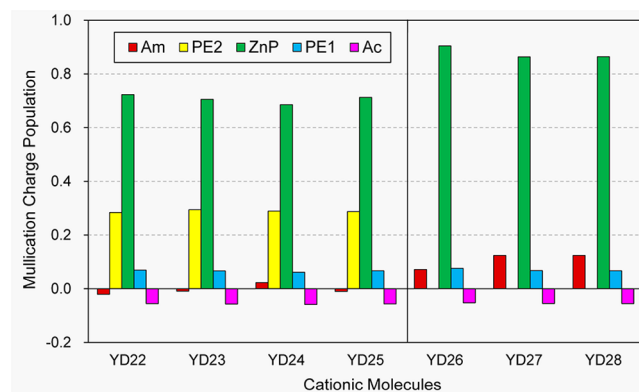


Figure 6. Cationic Mulliken charge population for YD-series dyes.

Mulliken charges for each fragment in the cationic dye are included. According to the results, the Am group does not help stabilizing the cationic charge significantly. To our surprise, the



ZnP unit possesses the highest positive charge among all the other fragments including amine donor. The charge for ZnP unit is 0.69–0.72 for dyes YD22–YD25 and 0.86–0.90 for YD26–YD28. This indicates that ZnP also tends to accumulate more cationic charge than the Am group. We note that for dyes YD22–YD25 the PE2 units can also accumulate positive charge density (0.28–0.29) in addition to ZnP unit. In other words, the positive charge can be stabilized at a distance away from TiO<sub>2</sub> surface such that charge recombination from TiO<sub>2</sub> to oxidized dye is less accessible. In addition, dye regeneration via approach of a redox mediator is less hindered by sterically demanding octyloxy chains on *meso*-phenyl groups of ZnP in a close proximity. Therefore, the insertion of a PE group at proper position is believed to be helpful to the device performance. Interestingly, PE2 is unable to stabilize the positive charge if positioned between ZnP and pull, as shown in a test with the regioisomer YD25', where the Mulliken charge of PE2 unit decreases from 0.29 to 0.04 (Figure S2). A comparison of structurally similar dyes LD21<sup>70</sup> ( $V_{OC} = 0.68$  V,  $J_{SC} = 12.92$  mA cm<sup>-2</sup>;  $\eta = 6.3\%$ ) and LAC-1<sup>34</sup> ( $V_{OC} = 0.67$  V,  $J_{SC} = 6.13$  mA cm<sup>-2</sup>;  $\eta = 3.0\%$ ) leads to better device performance of the former (in a form of R-PE2-ZnP-PE1-Ac; R = aryl group) than the latter (in a form of R-ZnP-PE2-PE1-Ac), showing the importance of implanted PE2 position.

## 4. CONCLUSIONS

The porphyrin dyes YD22–28 were synthesized and their photophysical and electrochemical properties and device characteristics were studied. The additional phenylethynylene (PE) in dyes YD22–YD25 results in red-shifted and intense Q-band absorption compared to that of PE-free dyes YD26–YD28. The first and second oxidation potentials of neutral dyes correspond to electron abstraction from both the arylamine donor (Am) and zinc porphyrin (ZnP) unit. Insertion of PE unit bridged between Am and ZnP leads to stabilization of HOMO level, as shown in the case of YD24 versus YD27 for bis(*p*-tolyl)-substituted amine donor as well as YD25 versus YD26 for diphenylamine donor. The PE unit also increases the injection probability of dyes YD22–YD25 by means of doubled absorption coefficient for Q-band transition. After charge injection, the positive charge of the dye molecule is mainly stabilized by the ZnP unit. The insertion of an additional PE unit at a proper position also plays crucial role in stabilizing the cationic charge. Examination via natural transition orbitals (NTOs) and Mulliken charge population analysis concludes that dyes based on Am-PE2-ZnP-PE1-Ac structure yield higher device performance than those based on Am-ZnP-PE1-Ac and Am-ZnP-PE2-PE1-Ac structures. Our analysis is based on a gas-phase model of a single dye molecule. In the real device system, more factors should be considered because the dyes are directly attached to the TiO<sub>2</sub> surface and are surrounded by solvent and electrolytes and can possibly interact with each other. Nevertheless, this study has provided valuable information about rational design for a push–pull-type porphyrin dye system.

## ■ ASSOCIATED CONTENT

### Supporting Information

The Supporting Information is available free of charge on the ACS Publications website at DOI: 10.1021/acsami.5b11554.

Syntheses of porphyrin dyes, additional electrochemical data, and theoretical calculation results. (PDF)

## ■ AUTHOR INFORMATION

### Corresponding Authors

\*E-mail: diau@mail.nctu.edu.tw.

\*E-mail: cherri@gate.sinica.edu.tw.

\*E-mail: cyeh@dragon.nchu.edu.tw.

### Notes

The authors declare no competing financial interest.

## ■ ACKNOWLEDGMENTS

We acknowledge the support from Ministry of Science and Technology and Ministry of Education, Taiwan.

## ■ REFERENCES

- (1) O'Regan, B.; Grätzel, M. A Low-Cost, High-Efficiency Solar Cell Based on Dye-Sensitized Colloidal TiO<sub>2</sub> Films. *Nature* **1991**, *353*, 737–740.
- (2) Hagfeldt, A.; Boschloo, G.; Sun, L.; Kloo, L.; Pettersson, H. Dye-Sensitized Solar Cells. *Chem. Rev.* **2010**, *110*, 6595–6663.
- (3) Cao, Y.; Bai, Y.; Yu, Q.; Cheng, Y.; Liu, S.; Shi, D.; Gao, F.; Wang, P. Dye-Sensitized Solar Cells with a High Absorptivity Ruthenium Sensitizer Featuring a 2-(Hexylthio)thiophene Conjugated Bipyridine. *J. Phys. Chem. C* **2009**, *113* (15), 6290–6297.
- (4) Grätzel, M. Photoelectrochemical Cells. *Nature* **2001**, *414*, 338–344.
- (5) Hagfeldt, A.; Grätzel, M. Molecular Photovoltaics. *Acc. Chem. Res.* **2000**, *33*, 269–277.
- (6) Hamann, T. W.; Jensen, R. A.; Martinson, A. B. F.; Van Ryswyk, H.; Hupp, J. T. Advancing Beyond Current Generation Dye-Sensitized Solar Cells. *Energy Environ. Sci.* **2008**, *1* (1), 66–78.
- (7) Yen, Y.-S.; Chou, H.-H.; Chen, Y.-C.; Hsu, C.-Y.; Lin, J. T. Recent Developments in Molecule-Based Organic Materials for Dye-Sensitized Solar Cells. *J. Mater. Chem.* **2012**, *22* (18), 8734–8747.
- (8) Liang, M.; Chen, J. Arylamine Organic Dyes for Dye-Sensitized Solar Cells. *Chem. Soc. Rev.* **2013**, *42* (8), 3453–3488.
- (9) Lee, C.-P.; Lin, R. Y.-Y.; Lin, L.-Y.; Li, C.-T.; Chu, T.-C.; Sun, S.-S.; Lin, J. T.; Ho, K.-C. Recent Progress in Organic Sensitizers for Dye-Sensitized Solar Cells. *RSC Adv.* **2015**, *5* (30), 23810–23825.
- (10) Balaban, T. S. Tailoring Porphyrins and Chlorins for Self-Assembly in Biomimetic Artificial Antenna Systems. *Acc. Chem. Res.* **2005**, *38*, 612–623.
- (11) Campbell, W. M.; Burrell, A. K.; Officer, D. L.; Jolley, K. W. Porphyrins as Light Harvesters in the Dye-Sensitized TiO<sub>2</sub> Solar Cell. *Coord. Chem. Rev.* **2004**, *248* (13–14), 1363–1379.
- (12) Imahori, H. Giant Multiporphyrin Arrays as Artificial Light-Harvesting Antennas. *J. Phys. Chem. B* **2004**, *108*, 6130–6143.
- (13) Panda, M. K.; Ladomenou, K.; Coutsolelos, A. G. Porphyrins in Bio-Inspired Transformations: Light-Harvesting to Solar Cell. *Coord. Chem. Rev.* **2012**, *256* (21–22), 2601–2627.
- (14) Urbani, M.; Grätzel, M.; Nazeeruddin, M. K.; Torres, T. Meso-Substituted Porphyrins for Dye-Sensitized Solar Cells. *Chem. Rev.* **2014**, *114* (24), 12330–12396.
- (15) Li, L. L.; Diau, E. W. Porphyrin-Sensitized Solar Cells. *Chem. Soc. Rev.* **2013**, *42* (1), 291–304.
- (16) Imahori, H.; Umeyama, T.; Ito, S. Large  $\pi$ -Aromatic Molecules as Potential Sensitizers for Highly Efficient Dye-Sensitized Solar Cells. *Acc. Chem. Res.* **2009**, *42*, 1809–1818.
- (17) Yella, A.; Lee, H.-W.; Tsao, H. N.; Yi, C.; Chandiran, A. K.; Nazeeruddin, M. K.; Diau, E. W.-G.; Yeh, C.-Y.; Zakeeruddin, S. M.; Grätzel, M. Porphyrin-Sensitized Solar Cells with Cobalt (II/III)-Based Redox Electrolyte Exceed 12% Efficiency. *Science* **2011**, *334* (6056), 629–634.
- (18) Mathew, S.; Yella, A.; Gao, P.; Humphry-Baker, R.; Curchod, B. F.; Ashari-Astani, N.; Tavernelli, I.; Rothlisberger, U.; Nazeeruddin, M. K.; Grätzel, M. Dye-Sensitized Solar Cells with 13% Efficiency Achieved Through the Molecular Engineering of Porphyrin Sensitizers. *Nat. Chem.* **2014**, *6* (3), 242–247.



- (19) Yella, A.; Mai, C.-L.; Zakeeruddin, S. M.; Chang, S.-N.; Hsieh, C.-H.; Yeh, C.-Y.; Grätzel, M. Molecular Engineering of Push-Pull Porphyrin Dyes for Highly Efficient Dye-Sensitized Solar Cells: The Role of Benzene Spacers. *Angew. Chem., Int. Ed.* **2014**, *53* (11), 2973–2977.
- (20) Koumura, N.; Wang, Z.-S.; Mori, S.; Miyashita, M.; Suzuki, E.; Hara, K. Alkyl-Functionalized Organic Dyes for Efficient Molecular Photovoltaics. *J. Am. Chem. Soc.* **2006**, *128* (44), 14256–14257.
- (21) Wang, Z.-S.; Koumura, N.; Cui, Y.; Takahashi, M.; Sekiguchi, H.; Mori, A.; Kubo, T.; Furube, A.; Hara, K. Hexylthiophene-Functionalized Carbazole Dyes for Efficient Molecular Photovoltaics: Tuning of Solar-Cell Performance by Structural Modification. *Chem. Mater.* **2008**, *20* (12), 3993–4003.
- (22) Hsieh, C.-P.; Lu, H.-P.; Chiu, C.-L.; Lee, C.-W.; Chuang, S.-H.; Mai, C.-L.; Yen, W.-N.; Hsu, S.-J.; Diao, E. W.-G.; Yeh, C.-Y. Synthesis and Characterization of Porphyrin Sensitizers with Various Electron-Donating Substituents for Highly Efficient Dye-Sensitized Solar Cells. *J. Mater. Chem.* **2010**, *20*, 1127–1134.
- (23) Lee, C.-W.; Lu, H.-P.; Lan, C.-M.; Huang, Y.-L.; Liang, Y.-R.; Yen, W.-N.; Liu, Y.-C.; Lin, Y.-S.; Diao, E. W.-G.; Yeh, C.-Y. Novel Zinc Porphyrin Sensitizers for Dye-Sensitized Solar Cells: Synthesis and Spectral, electrochemical, and Photovoltaic Properties. *Chem. - Eur. J.* **2009**, *15*, 1403–1412.
- (24) Lu, H. P.; Mai, C. L.; Tsia, C. Y.; Hsu, S. J.; Hsieh, C. P.; Chiu, C. L.; Yeh, C. Y.; Diao, E. W. Design and Characterization of Highly Efficient Porphyrin Sensitizers for Green See-Through Dye-Sensitized Solar Cells. *Phys. Chem. Chem. Phys.* **2009**, *11* (44), 10270–10274.
- (25) Lu, H.-P.; Tsai, C.-Y.; Yen, W.-N.; Hsieh, C.-P.; Lee, C.-W.; Yeh, C.-Y.; Diao, E. W.-G. Control of Dye Aggregation and Electron Injection for Highly Efficient Porphyrin Sensitizers Adsorbed on Semiconductor Films with Varying Ratios of Coadsorbate. *J. Phys. Chem. C* **2009**, *113* (49), 20990–20997.
- (26) Kurotobi, K.; Toude, Y.; Kawamoto, K.; Fujimori, Y.; Ito, S.; Chabera, P.; Sundstrom, V.; Imahori, H. Highly Asymmetrical Porphyrins with Enhanced Push-Pull Character for Dye-Sensitized Solar Cells. *Chem. - Eur. J.* **2013**, *19* (50), 17075–17081.
- (27) Wu, C.-H.; Chen, M.-C.; Su, P.-C.; Kuo, H.-H.; Wang, C.-L.; Lu, C.-Y.; Tsai, C.-H.; Wu, C.-C.; Lin, C.-Y. Porphyrins for Efficient Dye-Sensitized Solar Cells Covering the Near-IR Region. *J. Mater. Chem. A* **2014**, *2* (4), 991–999.
- (28) Qi, Q.; Li, R.; Luo, J.; Zheng, B.; Huang, K.-W.; Wang, P.; Wu, J. Push–Pull Type Porphyrin Based Sensitizers: The Effect of Donor Structure on the Light-Harvesting Ability and Photovoltaic Performance. *Dyes Pigm.* **2015**, *122*, 199–205.
- (29) van der Salm, H.; Lind, S. J.; Griffith, M. J.; Wagner, P.; Wallace, G. G.; Officer, D. L.; Gordon, K. C. Probing Donor-Acceptor Interactions in meso-Substituted Zn(II) Porphyrins Using Resonance Raman Spectroscopy and Computational Chemistry. *J. Phys. Chem. C* **2015**, *119*, 22379.
- (30) Bessho, T.; Zakeeruddin, S. M.; Yeh, C. Y.; Diao, E. W.; Grätzel, M. Highly Efficient Mesoscopic Dye-Sensitized Solar Cells Based on Donor-Acceptor-Substituted Porphyrins. *Angew. Chem., Int. Ed.* **2010**, *49* (37), 6646–6649.
- (31) Wu, S.-L.; Lu, H.-P.; Yu, H.-T.; Chuang, S.-H.; Chiu, C.-L.; Lee, C.-W.; Diao, E. W.-G.; Yeh, C.-Y. Design and Characterization of Porphyrin Sensitizers with a Push-Pull Framework for Highly Efficient Dye-Sensitized Solar Cells. *Energy Environ. Sci.* **2010**, *3* (7), 949–955.
- (32) Chang, Y.-C.; Wang, C.-L.; Pan, T.-Y.; Hong, S.-H.; Lan, C.-M.; Kuo, H.-H.; Lo, C.-F.; Hsu, H.-Y.; Lin, C.-Y.; Diao, E. W.-G. A Strategy to Design Highly Efficient Porphyrin Sensitizers for Dye-Sensitized Solar Cells. *Chem. Commun.* **2011**, *47* (31), 8910–8912.
- (33) Lee, C.-Y.; Hupp, J. T. Dye Sensitized Solar Cells: TiO<sub>2</sub> Sensitization with a Bodipy-Porphyrin Antenna System. *Langmuir* **2010**, *26* (5), 3760–3765.
- (34) Lin, C.-Y.; Wang, Y.-C.; Hsu, S.-J.; Lo, C.-F.; Diao, E. W.-G. Preparation and Spectral, Electrochemical, and Photovoltaic Properties of Acene-Modified Zinc Porphyrins. *J. Phys. Chem. C* **2010**, *114*, 687–693.
- (35) Wei, T.; Sun, X.; Li, X.; Agren, H.; Xie, Y. Systematic Investigations on the Roles of the Electron Acceptor and Neighboring Ethynylene Moiety in Porphyrins for Dye-Sensitized Solar Cells. *ACS Appl. Mater. Interfaces* **2015**, *7*, 21956–21965.
- (36) Shiu, J.-W.; Chang, Y.-C.; Chan, C.-Y.; Wu, H.-P.; Hsu, H.-Y.; Wang, C.-L.; Lin, C.-Y.; Diao, E. W.-G. Panchromatic Co-Sensitization of Porphyrin-Sensitized Solar Cells to Harvest Near-Infrared Light Beyond 900 nm. *J. Mater. Chem. A* **2015**, *3* (4), 1417–1420.
- (37) Xie, Y.; Tang, Y.; Wu, W.; Wang, Y.; Liu, J.; Li, X.; Tian, H.; Zhu, W. H. Porphyrin Cosensitization for a Photovoltaic Efficiency of 11.5%: A Record for Non-Ruthenium Solar Cells Based on Iodine Electrolyte. *J. Am. Chem. Soc.* **2015**, *137* (44), 14055–8.
- (38) Wang, C.-L.; Shiu, J.-W.; Hsiao, Y.-N.; Chao, P.-S.; Wei-Guang Diao, E.; Lin, C.-Y. Co-Sensitization of Zinc and Free-Base Porphyrins with an Organic Dye for Efficient Dye-Sensitized Solar Cells. *J. Phys. Chem. C* **2014**, *118* (48), 27801–27807.
- (39) Yeh, C.-Y.; Lee, H.-W.; Ou, T. W.; Wang, L.-H.; Guo, B.-C.; Mai, C.-L.; Chen, J.-G. Green Zinc Porphyrin Sensitizers and Their Applications. U.S. Pat. 0090469A1, 2013.
- (40) Shao, Y.; Molnar, L. F.; Jung, Y.; Kussmann, J.; Ochsenfeld, C.; Brown, S. T.; Gilbert, A. T.; Slipchenko, L. V.; Levchenko, S. V.; O'Neill, D. P.; et al. Advances in Methods and Algorithms in A Modern Quantum Chemistry Program Package. *Phys. Chem. Chem. Phys.* **2006**, *8* (27), 3172–3191.
- (41) Rohrdanz, M. A.; Martins, K. M.; Herbert, J. M. A Long-Range-Corrected Density Functional that Performs Well for both Ground-State Properties and Time-Dependent Density Functional Theory Excitation Energies, Including Charge-Transfer Excited States. *J. Chem. Phys.* **2009**, *130* (5), 054112.
- (42) Rohrdanz, M. A.; Herbert, J. M. Simultaneous Benchmarking of Ground- and Excited-State Properties with Long-Range-Corrected Density Functional Theory. *J. Chem. Phys.* **2008**, *129* (3), 034107.
- (43) You, Z.-Q.; Hung, Y.-C.; Hsu, C.-P. Calculating Electron-Transfer Coupling with Density Functional Theory: The Long-Range-Corrected Density Functionals. *J. Phys. Chem. B* **2015**, *119* (24), 7480–7490.
- (44) Chen, Y.-C.; Chou, H.-H.; Tsai, M. C.; Chen, S.-Y.; Lin, J. T.; Yao, C.-F.; Chen, K. Thieno[3,4-*b*]thiophene-Based Organic Dyes for Dye-Sensitized Solar Cells. *Chem. - Eur. J.* **2012**, *18* (17), 5430–5437.
- (45) Chou, H.-H.; Chen, Y.-C.; Huang, H.-J.; Lee, T.-H.; Lin, J. T.; Tsai, C.; Chen, K. High-Performance Dye-Sensitized Solar Cells Based on 5,6-Bis-Hexyloxy-Benzo[2,1,3]thiadiazole. *J. Mater. Chem.* **2012**, *22* (21), 10929.
- (46) Huang, S.-T.; Hsu, Y.-C.; Yen, Y.-S.; Chou, H.-H.; Lin, J. T.; Chang, C.-W.; Hsu, C.-P.; Tsai, C.; Yin, D.-J. Organic Dyes Containing a Cyanovinyl Entity in the Spacer for Solar Cells Applications. *J. Phys. Chem. C* **2008**, *112*, 19739–19747.
- (47) Lee, C.-W.; Lu, H.-P.; Reddy, N. M.; Lee, H.-W.; Diao, E. W.-G.; Yeh, C.-Y. Electronically Coupled Porphyrin-Arene Dyads for Dye-Sensitized Solar Cells. *Dyes Pigm.* **2011**, *91* (3), 317–323.
- (48) Sonogashira, K.; Tohda, Y.; Hagihara, N. A Convenient Synthesis of Acetylenes: Catalytic Substitutions of Acetylenic Hydrogen with Bromoalkenes, Iodoarenes and Bromopyridines. *Tetrahedron Lett.* **1975**, *16* (50), 4467–4470.
- (49) Hartwig, J. F. Transition Metal Catalyzed Synthesis of Arylamines and Aryl Ethers from Aryl Halides and Triflates: Scope and Mechanism. *Angew. Chem., Int. Ed.* **1998**, *37* (15), 2046–2067.
- (50) Wolfe, J. P.; Wagaw, S.; Marcoux, J.-F.; Buchwald, S. L. Rational Development of Practical Catalysts for Aromatic Carbon-Nitrogen Bond Formation. *Acc. Chem. Res.* **1998**, *31*, 805–818.
- (51) Spellane, P. J.; Gouterman, M.; Antipas, A.; Kim, S.; Liu, Y. C. Porphyrins. 40. Electronic Spectra and Four-Orbital Energies of Free-Base, Zinc, Copper, and Palladium Tetrakis(perfluorophenyl)-porphyrins. *Inorg. Chem.* **1980**, *19*, 386–391.
- (52) Chou, H.-H.; Hsu, C.-Y.; Hsu, Y.-C.; Lin, Y.-S.; Lin, J. T.; Tsai, C. Dipolar Organic Pyridyl Dyes for Dye-Sensitized Solar Cell Applications. *Tetrahedron* **2012**, *68* (2), 767–773.
- (53) Hagberg, D. P.; Edvinsson, T.; Marinado, T.; Boschloo, G.; Hagfeldt, A.; Sun, L. A Novel Organic Chromophore for Dye-

Sensitized Nanostructured Solar Cells. *Chem. Commun.* **2006**, *21*, 2245–2247.

(54) Urbani, M.; Barea, E. M.; Trevisan, R.; Aljarilla, A.; de la Cruz, P.; Bisquert, J.; Langa, F. A Star-Shaped Sensitizer Based on Thiophylenevinylene for Dye-Sensitized Solar Cells. *Tetrahedron Lett.* **2013**, *54* (5), 431–435.

(55) Chen, R.; Yang, X.; Tian, H.; Wang, X.; Hagfeldt, A.; Sun, L. Effect of Tetrahydroquinoline Dyes Structure on the Performance of Organic Dye-Sensitized Solar Cells. *Chem. Mater.* **2007**, *19*, 4007–4015.

(56) Wang, M.; Xu, M.; Shi, D.; Li, R.; Gao, F.; Zhang, G.; Yi, Z.; Humphry-Baker, R.; Wang, P.; Zakeeruddin, S. M.; et al. High-Performance Liquid and Solid Dye-Sensitized Solar Cells Based on a Novel Metal-Free Organic Sensitizer. *Adv. Mater.* **2008**, *20* (23), 4460–4463.

(57) Xu, M.; Li, R.; Pootrakulchote, N.; Shi, D.; Guo, J.; Yi, Z.; Zakeeruddin, S. M.; Grätzel, M.; Wang, P. Energy-Level and Molecular Engineering of Organic D- $\pi$ -A Sensitizers in Dye-Sensitized Solar Cells. *J. Phys. Chem. C* **2008**, *112* (49), 19770–19776.

(58) Clifford, J. N.; Martínez-Ferrero, E.; Palomares, E. Dye Mediated Charge Recombination Dynamics in Nanocrystalline TiO<sub>2</sub> Dye Sensitized Solar Cells. *J. Mater. Chem.* **2012**, *22* (25), 12415–12422.

(59) Fabregat-Santiago, F.; Garcia-Belmonte, G.; Mora-Sero, I.; Bisquert, J. Characterization of Nanostructured Hybrid and Organic Solar Cells by Impedance Spectroscopy. *Phys. Chem. Chem. Phys.* **2011**, *13* (20), 9083–9118.

(60) Luo, J.; Xu, M.; Li, R.; Huang, K. W.; Jiang, C.; Qi, Q.; Zeng, W.; Zhang, J.; Chi, C.; Wang, P.; et al. N-Annulated Perylene as an Efficient Electron Donor for Porphyrin-Based Dyes: Enhanced Light-Harvesting Ability and High-Efficiency Co(II/III)-Based Dye-Sensitized Solar Cells. *J. Am. Chem. Soc.* **2014**, *136* (1), 265–272.

(61) Stergiopoulos, T.; Falaras, P. Minimizing Energy Losses in Dye-Sensitized Solar Cells Using Coordination Compounds as Alternative Redox Mediators Coupled with Appropriate Organic Dyes. *Adv. Energy Mater.* **2012**, *2* (6), 616–627.

(62) Barnes, P. R.; Miettunen, K.; Li, X.; Anderson, A. Y.; Bessho, T.; Grätzel, M.; O'Regan, B. C. Interpretation of Optoelectronic Transient and Charge Extraction Measurements in Dye-Sensitized Solar Cells. *Adv. Mater.* **2013**, *25* (13), 1881–922.

(63) Li, L.-L.; Chang, Y.-C.; Wu, H.-P.; Diau, E. W.-G. Characterisation of Electron Transport and Charge Recombination Using Temporally Resolved and Frequency-Domain Techniques for Dye-Sensitized Solar Cells. *Int. Rev. Phys. Chem.* **2012**, *31* (3), 420–467.

(64) Martin, R. L. Natural Transition Orbitals. *J. Chem. Phys.* **2003**, *118* (11), 4775–4777.

(65) Gurzadyan, G. G.; Tran-Thi, T.-H.; Gustavsson, T. Time-Resolved Fluorescence Spectroscopy of High-Lying Electronic States of Zn-Tetraphenylporphyrin. *J. Chem. Phys.* **1998**, *108* (2), 385–388.

(66) Liu, X.; Tripathy, U.; Bhosale, S. V.; Langford, S. J.; Steer, R. P. Photophysics of Soret-Excited Tetrapyrroles in Solution. II. Effects of Perdeuteration, Substituent Nature and Position, and Macrocyclic Structure and Conformation in Zinc(II) Porphyrins. *J. Phys. Chem. A* **2008**, *112*, 8986–8998.

(67) Yu, H.-Z.; Baskin, J. S.; Zewail, A. H. Ultrafast Dynamics of Porphyrins in the Condensed Phase: II. Zinc Tetraphenylporphyrin. *J. Phys. Chem. A* **2002**, *106*, 9845–9854.

(68) Chen, C.-H.; Hsu, Y.-C.; Chou, H.-H.; Thomas, K. R. J.; Lin, J. T.; Hsu, C.-P. Dipolar Compounds Containing Fluorene and a Heteroaromatic Ring as the Conjugating Bridge for High-Performance Dye-Sensitized Solar Cells. *Chem. - Eur. J.* **2010**, *16* (10), 3184–3193.

(69) Pastore, M.; Fantacci, S.; De Angelis, F. Modeling Excited States and Alignment of Energy Levels in Dye-Sensitized Solar Cells: Successes, Failures, and Challenges. *J. Phys. Chem. C* **2013**, *117* (8), 3685–3700.

(70) Wu, C.-H.; Pan, T.-Y.; Hong, S.-H.; Wang, C.-L.; Kuo, H.-H.; Chu, Y.-Y.; Diau, E. W.-G.; Lin, C.-Y. A Fluorene-Modified Porphyrin for Efficient Dye-Sensitized Solar Cells. *Chem. Commun.* **2012**, *48* (36), 4329–4331.